Altered Nuclear Receptor Corepressor Expression Attenuates Vitamin D Receptor Signaling in Breast Cancer Cells

Claire M. Banwell,[1] Donia P. MacCartney,[1] Michelle Guy,[4] Alice E. Miles,[1] Milan R. Uskokovic,[3] Janine Mansi,[4] Paul M. Stewart,[1] Laura P. O'Neill,[2] Bryan M. Turner,[2] Kay W. Colston,[4] and Moray J. Campbell[1]

Abstract

Purpose: We hypothesized that deregulated corepressor actions, with associated histone deacetylation activity, epigenetically suppressed vitamin D receptor (VDR) responsiveness and drives resistance towards 1α,25-dihydroxyvitamin D_3.

Experimental Design: Profiling, transcriptional, and proliferation assays were undertaken in $1\alpha,25(OH)_2D_3$-sensitive MCF-12A nonmalignant breast epithelial cells, a panel of breast cancer cell lines, and a cohort of primary breast cancer tumors ($n = 21$).

Results: Elevated *NCoR1* mRNA levels correlated with suppressed regulation of VDR target genes and the ability of cells to undergo arrest in G_1 of the cell cycle. A similar increased ratio of corepressor mRNA to *VDR* occurred in matched primary tumor and normal cells, noticeably in estrogen receptor α – negative ($n = 7$) tumors. $1\alpha,25(OH)_2D_3$ resistance in cancer cell lines was targeted by cotreatments with either $1\alpha,25(OH)_2D_3$ or a metabolically stable analogue (RO-26-2198) in combination with either trichostatin A (TSA; histone deacetylation inhibitor) or 5-aza-2′-deoxycytidine (DNA methyltransferase inhibitor). Combinations of vitamin D_3 compounds with TSA restored VDR antiproliferative signaling (target gene regulation, cell cycle arrest, and antiproliferative effects in liquid culture) to levels which were indistinguishable from MCF-12A cells.

Conclusions: Increased *NCoR1* mRNA is a novel molecular lesion in breast cancer cells, which acts to suppress responsiveness of VDR target genes, resulting in $1\alpha,25(OH)_2D_3$ resistance and seems to be particularly associated with estrogen receptor negativity. This lesion provides a novel molecular diagnostic and can be targeted by combinations of vitamin D_3 compounds and low doses of TSA.

The nuclear receptor superfamily regulates diverse signals that are central to the formation and homeostasis of the mammary gland. The postgenomic description of the superfamily conjoined with profiling approaches (1) reveals that breast myoepithelial and epithelial cells express a rich cohort of nuclear receptors, many of which display overt nutrient-sensing capacity for micronutrients and macronutrients alongside the estrogen receptors (ERα and ERβ; refs. 2–6).

Several of the diet-sensing nuclear receptors, such as the VDR, preferentially form heterodimers with retinoid X receptors whereas the ERs preferentially heterodimerize with one another. For the nuclear receptors to regulate transcriptional programs, these dimers must be contained as subunits in either large gene coactivator or corepressor complexes. In the absence of ligand, receptors exist in an *apo* state as part of large complexes (~2.0 MDa; ref. 7), associated with corepressors (e.g., NCoR1, NCoR2/SMRT, and TRIP15/Alien), and bound to response element sequences. These complexes actively recruit a range of enzymes that posttranslationally modify histone tails (e.g., histone deacetylases and methyltransferases) and thereby maintain a locally closed chromatin structure around response element sequences (8). Ligand binding induces a so-called *holo* receptor state, facilitating the association of the receptor dimer with coactivator complexes. These receptor coactivator complexes coordinate the recruitment of an antagonistic battery of enzymes and induce the reorganization of local chromatin to facilitate gene transcription (9–11). Thus, cofactor expression is critical to determine cellular sensitivity to ligand although the specificity of receptor and either coactivator or corepressor interactions remains to be established fully.

In vivo studies on *vdr* knockout mice show the requirement for 1α,25-dihydroxyvitamin D_3 [$1\alpha,25(OH)_2D_3$] for mammary gland function and differentiation (12). Parallel studies by ourselves and others have found epidemiologic links between the incidence of breast cancers and low serum $25(OH)D_3$ levels (13, 14); the risk is compounded by specific VDR polymorphisms (15, 16). *In vitro* studies show that MDA-MB-231 and other cancer cells show a spectrum of insensitivity toward $1\alpha,25(OH)_2D_3$ (17, 18). Taken together, these data suggest that functional VDR-mediated signaling is required for correct gland function and that $1\alpha,25(OH)_2D_3$-deficient environments

Authors' Affiliations: [1]Institute of Biomedical Research, Endocrinology and Metabolism and [2]Division of Immunity and Infection, University of Birmingham Medical School, Edgbaston, Birmingham, United Kingdom; [3]Hoffman La Roche, Nutley, New Jersey; and [4]Department of Clinical Biochemistry, St. George's Hospital Medical School, London, United Kingdom

Received 6/6/05; revised 11/17/05; accepted 1/26/06.

The costs of publication of this article were defrayed in part by the payment of page charges. This article must therefore be hereby marked *advertisement* in accordance with 18 U.S.C. Section 1734 solely to indicate this fact.

Requests for reprints: Moray J. Campbell, Institute of Biomedical Research, Endocrinology and Metabolism, University of Birmingham Medical School, Wolfson Drive, Edgbaston, Birmingham, United Kingdom. Phone: 44-121-415-8713; Fax: 011-44-121-415-8712; E-mail: m.j.campbell@bham.ac.uk.

doi:10.1158/1078-0432.CCR-05-1218

and/or cellular mechanisms which suppress sensitivity to $1\alpha,25(OH)_2D_3$ are both associated with malignancy. The mechanisms for cellular $1\alpha,25(OH)_2D_3$ insensitivity in breast cancer are as yet unclear and limit therapeutic applications, although a lack of a functional VDR alone cannot explain resistance (17, 19).

We have previously proposed and investigated epigenetic mechanisms as the basis for corruption of VDR signaling in prostate cancer (20, 21). In the current study, we have used these findings for the basis of investigation of nuclear receptor corepressor expression and activity to derive breast cancer insensitivity towards $1\alpha,25(OH)_2D_3$. By contrast, other workers have suggested that *NCoR1* is down-regulated in ERα-positive breast cancers as a mechanism of escaping endocrine restraint by tamoxifen (22–25). It thus remains to be resolved which are the pivotal interactions of corepressors, either to drive insensitivity to antimitotic receptors such as the VDR or to play a role in evolving tamoxifen resistance. In the current study, we have investigated the potential for corepressor-mediated mechanisms to attenuate VDR signaling pathways in both ERα-positive and ERα-negative cell line and tumor backgrounds.

Materials and Methods

Vitamin D_3 compounds and epigenetic inhibitors. $1\alpha,25(OH)_2D_3$ and a potent analogue that is resistant to CYP24 metabolism, 1α,25-dihydroxy-16,23Z-diene-26,27-hexafluoro-19-nor vitamin D_3 (RO-26-2198; refs. 26–31), trichostatin A (TSA), and 5-aza-2′-deoxycytidine (5-aza-dCyd; Sigma, Poole, United Kingdom) were all stored as 1 mmol/L stock solutions in ethanol at −20°C.

Cell culture. The breast cancer cell lines T-47D, ZR-75-1, MCF-7, and MDA-MB-231 were supplemented with 100 units/mL penicillin, 100 μg/mL streptomycin, and 10% fetal bovine serum (Life Technologies, Inc., Paisley) in RPMI medium and passaged by trypsinizing with trypsin-EDTA (Life Technologies). MCF-12A cells were a generous gift of Prof. H. Phillip Koeffler (Cedars-Sinai Medical Ctr/University of California at Los Angeles School of Medicine, Los Angeles, CA). These cells are a nontumorigenic epithelial cell line established from tissue taken at reduction mammoplasty from a nulliparous patient with fibrocystic breast disease that contained focal areas of intraductal hyperplasia (32). They are not tumorigenic in immunosuppressed mice but do form colonies in semisolid medium. These cells were cultured in a 1:1 mixture of DMEM and Ham's F12 medium, 20 ng/mL epidermal growth factor, 100 ng/mL cholera toxin, 0.01 mg/mL insulin and 500 ng/mL hydrocortisone, 95%; horse serum, 5%. All cells were grown at 37°C in a humidified atmosphere of 5% CO_2 in air.

mRNA from tumor panels. Matched tumor and normal tissues were obtained from biopsies/resection specimens of Caucasian female patients who had undergone surgery for invasive ductal breast cancer at St. George's Hospital (London, United Kingdom). Age at diagnosis of primary tumor (range, 35-88 years) and estrogen receptor status were validated from histopathologic reports and patient medical records. The study received local ethical approval from St. George's Hospital Medical School Ethics Committee. Total RNA was extracted using the RNeasy and the Lipid Tissue Mini Kit (Qiagen, Crawley, United Kingdom). Briefly, a piece of breast tissue, ~2 mm^3 in size, was excised from the relevant frozen surgical sample, which had been stored in liquid nitrogen. The tissue was placed directly into 1 mL of lysis reagent and homogenized using a rotor-stator homogenizer (IKA-Werke, Staufen, Germany). Total RNA was then extracted according to the instructions of the manufacturer, with one modification: before ethanol washes, DNA digestion was carried out using RQ1 Rnase-Free DNase (Promega, Southampton, United Kingdom) by the addition of 10 μL of RQ1 DNase, 10 μL of 10× RQ1 buffer, and 80 μL of H_2O to each column, followed by 15-minute incubation at room temperature. RNA was eluted in 30 μL of RNase-free water and stored at −70°C.

Liquid proliferation assay. The action of individual agents alone and in combination was examined using a bioluminescent technique to measure changes in liberated cellular ATP per treatment well (ViaLight HS, LumiTech, Nottingham, United Kingdom), with previously optimized conditions, according to the instructions of the manufacturer. This assay has proved to yield a linear relationship between ATP levels in a test well and a wide range of cell numbers. Therefore, inhibition of proliferation can be readily measured in test wells by measuring the decrease in ATP levels relative to untreated wells (20).

Briefly, cells were plated in 96-well white-walled tissue culture treated plates (Fisher Scientific Ltd., Loughborough, United Kingdom) at either 2×10^3 per well (MCF-7 and MDA-MB-231) or 4×10^3 per well (MCF-12A, ZR-75-1, and T47-D). Growth media containing varying concentrations of 5-aza-dCyd, TSA, $1\alpha,25(OH)_2D_3$, and vitamin D_3 analogue were added to a final volume of 100 μL/well and the plates were incubated for 96 hours, with redosing after 48 hours. After the incubation period, 100 μL of nucleotide releasing reagent were added to each well and left for 15 minutes at room temperature. Liberated ATP was quantitated by adding 20 μL of ATP monitoring reagent (containing luciferin and luciferase) and measuring luminescence with a microplate luminometer (Berthold Detection Systems, Fisher Scientific). ATP levels were recorded in relative luciferase units and inhibition of proliferation was expressed as a percentage of control. All experiments were repeated in triplicate wells in three separate experiments.

Clonal proliferation in soft agar. Trypsinized and washed single-cell suspensions of cells from 80% confluent cultures were enumerated and plated into 24-well flat-bottomed plates (Costar, Bucks, United Kingdom) using a two-layer soft-agar system with a total of 1×10^3 cells per well in a total volume of 600 μL/well. Both layers were prepared with sterile agar (1%) that had been equilibrated previously at 42°C. TSA and/or $1\alpha,25(OH)_2D_3$ was added to the wells before the addition of the feeder layer (20% FCS, 40% 2× RPMI, 40% agar). The cells were mixed into the top layer [20% FCS, 30% 2× RPMI, 30% agar, 18% medium containing cells, 1% L-glutamine (100 mg/mL), 1% β-mercaptoethanol (1 mmol/L)] and plated onto the preset under layer. After 14 days of incubation at 37°C in a humidified atmosphere of CO_2 in air, the colonies (>50 cells) were counted under an inverted microscope. All experiments were done thrice in triplicate.

Cell cycle analysis. The effect on the cell cycle distribution of vitamin D_3 compounds, alone and in combination with TSA, was measured by staining cell DNA with propidium iodide. Briefly, T25 flasks were seeded with 2.5×10^5 subconfluent, exponentially proliferating cells, exposed to either agent at time 0 (and redosed after 48 hours in 72-hour assays). After a total of 24 and 72 hours, cultures were harvested, counted, and 1×10^6 cells were stained with propidium iodide buffer [10 μg/mL propidium iodide, 1% (w/v) trisodium citrate, 0.1% (v/v) Triton X-100, 100 μmol/L sodium chloride (Sigma)]. Cell cycle distribution was determined using a Becton Dickinson Flow Cytometer and CellFIT Cell Cycle Analysis software. Each condition was examined in triplicate experiments.

Quantitative reverse transcription-PCR. Cells were seeded at low and high densities ($2 \times 10^4/cm^2$ and $8 \times 10^4/cm^2$, respectively). The subconfluent cultures were harvested after 24 hours whereas the high-density cultures were cultured until reaching confluence (~48 hours). For treatment, the cells were seeded as subconfluent conditions and treated with fresh medium or vitamin D_3 compounds alone or in combination with TSA as indicated. Total RNA was extracted using the GenElute RNA extraction system (Sigma) according to the instructions of the manufacturer. The cDNA was prepared from RNA (1 μg) that was initially heated to 70°C for 5 minutes with 100 pmol random hexamers (Promega). The RNA was then added to an 18-μL reaction mix, which contained a final concentration of 10 units of avian myeloblastosis virus, 1× reaction buffer, 1 unit of RNase inhibitor, and 1 mmol/L

deoxynucleotide triphosphates. Each reaction was heated for 30 minutes at 37°C, followed by 5 minutes at 95°C.

Expression of specific mRNAs was quantitated using the ABI PRISM 7700 Sequence Detection System. Each sample was amplified in triplicate wells in 25-μL volumes containing 1× TaqMan Universal PCR Master Mix [3 mmol/L $Mn(OAc)_2$, 200 μmol/L deoxynucleotide triphosphates, 1.25 units AmpliTaq Gold polymerase, 1.25 units AmpErase UNG], 3.125 pmol FAM-labeled TaqMan probe, and 22.5 pmol primers. All reactions were multiplexed with preoptimized control primers to ensure parallel amplification with VIC-labeled probe for 18S rRNA (Perkin-Elmer Biosystems, Warrington, United Kingdom). Primer and probe sequences were previously described (20) and were designed for the current study [VDUP-1 forward primer, GCCTGCTGATTGTCATGGAA; VDUP-1 reverse primer, TGGTCTCCTCGATCCTGGAT; VDUP-1 probe, TTTGACGGTGGAGAACTCTTTAGCCGT] or were provided from Assay-on-Demand (cytokeratin 19, Perkin-Elmer Biosystems). Reactions were cycled as follows: 50°C for 2 minutes, 95°C for 10 minutes; then 44 cycles of 95°C for 15 seconds and 60°C for 1 minute. Data were expressed as Ct values (the cycle number at which logarithmic PCR plots cross a calculated threshold line) and used to determine δCt values (δCt = Ct of the target gene − Ct of the 18S). The data were transformed through the equation $2^{-\delta\delta Ct}$ to give fold changes in gene expression.

To exclude potential bias due to averaging of data, all statistics were done with δCt values. Measurements were carried out at least thrice in triplicate wells for each condition.

Western immunoblot analysis. Cells were seeded at low and high densities ($2 \times 10^4/cm^2$ and $8 \times 10^4/cm^2$, respectively) and either harvested after 24 hours (subconfluent) or cultured until the high-density cultures reached confluency (72 hours) to give subconfluent and confluent cultures, respectively. Whole-cell lysates were prepared at indicated time points and Western immunoblot analysis was done as previously described (17). Briefly, 30 μg of total protein for each sample were electrophoresed on an SDS-polyacrylamide gel, transferred onto polyvinylidene difluoride membrane (Immobilon-P, Millipore, Bedford, MA), and blocked with TBS-Tween 20 containing 5% milk powder for 1 hour. For detection of cyclin E, a rabbit polyclonal antibody (C4976, Sigma) was diluted 1:500. The secondary antibody was horseradish peroxidase conjugated (Amersham, Buckinghamshire, United Kingdom) and diluted 1:2,000. Proteins were detected using enhanced chemiluminescence (Amersham) and autoradiography. To ensure even loading and transfer of protein, membranes were stripped, washed for 15 minutes with TBS-Tween 20, and incubated at 1:5,000 dilution with primary mouse monoclonal β-actin antibody (AC-15, Sigma). An antimouse-horseradish peroxidase secondary antibody was used at 1:3,000 and signals were developed with enhanced chemiluminescence and autoradiography as described above. To quantify the relative changes in protein levels, densitometric analysis was done on the autoradiographs and values were normalized to β-actin levels.

Statistical analysis. The interactions of two compounds were assessed by measuring the mean effect of either compound acting alone (± SE; refs. 20, 21, 33). The combination of the mean effect for each compound acting alone was the predicted combined inhibition. The mean observed combined inhibition was then compared with this value using the Student's *t* test. Classification of the inhibitory effects were as follows: strong additive effects were those with an experimental value significantly greater than the predicted value; additive effects were those in which the experimental value did not significantly differ from the predicted value; and subadditive effects were those in which the experimental value was significantly less than the predicted value.

Results

Breast cancer cells show suppressed antiproliferative and gene-regulatory responses towards 1α,25(OH)$_2$D$_3$. To confirm the extent of the suppressed responsiveness towards $1\alpha,25(OH)_2D_3$, we compared the effect of $1\alpha,25(OH)_2D_3$ on the proliferation of a panel of breast cancer cell lines with that on nonmalignant MCF-12A cells using clonal proliferation in soft agar and liquid proliferation assays. MCF-12A cells were significantly and acutely inhibited with ED_{50} of ~20 and ~300 nmol/L in the soft-agar and liquid media, respectively (Table 1). Complete inhibition of clonal proliferation in soft agar was achieved at 100 nmol/L (ED_{90} = 70 nmol/L), but not in liquid proliferation assays. In contrast, the malignant cell lines displayed a spectrum of reduced sensitivities towards $1\alpha,25(OH)_2D_3$ (Table 1). T47-D was the most sensitive cell line, with an ED_{50} in colony formation assay comparable to that of MCF-12A, although it did not display an ED_{90} value. The remaining lines all showed greater ED_{50} values in soft agar than MCF-12A cells (Table 1). Indeed, MDA-MB-231 cells did not achieve an ED_{50} even at 1,000 nmol/L. The responses of the cancer cell lines towards $1\alpha,25(OH)_2D_3$ in the liquid proliferation assay were all suppressed, compared with MCF-12A cells, with ED_{50} values not being achieved.

In contrast to the differential sensitivity displayed by MCF-12A and the breast cancer cell lines towards $1\alpha,25(OH)_2D_3$, all cell lines displayed comparable and significant responses towards the histone deacetylation inhibitor TSA. The responses to the methytransferase inhibitor 5-aza-dCyd were more heterogeneous (Table 1).

In an attempt to characterize more fully the apparent insensitivity towards $1\alpha,25(OH)_2D_3$, we investigated the basal

Table 1. Cell sensitivities towards $1\alpha,25(OH)_2D_3$, TSA, and 5-aza-dCyd

Cell line	ED_{50}CP $1\alpha,25(OH)_2D_3$ (nmol/L)	ED_{50}LP $1\alpha,25(OH)_2D_3$ (nmol/L)	ED_{25}LP TSA (nmol/L)	ED_{50}LP TSA (nmol/L)	ED_{25}LP 5-aza-dCyd (nmol/L)	ED_{50}LP 5-aza-dCyd (nmol/L)
MCF-12A	20	300	25	40	85	130
T47-D	15	>1,000	10	45	110	>8,000
ZR-75-1	100	>1,000	35	100	740	>8,000
MCF-7	100	>1,000	25	45	65	1,825
MDA-MB-231	>100	>1,000	15	30	85	8,000

NOTE: Cellular responses were screened on two different assay formats, clonal proliferation (CP) in soft agar in 24-well plates and liquid proliferation (LP) in 96-well plates. The ED_{50} and ED_{25} were interpolated from dose-response graphs.

and regulated levels of the established VDR target genes *CYP24*, *GADD45α*, and *VDUP-1* in MCF-12A and MDA-MB-231 cells. During exponential proliferation, the basal levels of *CYP24* and *VDUP-1* were significantly elevated (78- and 4.3-fold, respectively; $P < 0.0001$) in MDA-MB-231 compared with MCF-12A cells whereas *GADD45α* did not significantly differ between cell types (data not shown).

The $1\alpha,25(OH)_2D_3$-mediated accumulation of target gene mRNA reflected the suppressed antiproliferative responses. Thus, in MCF-12A cells, there was a clear 60-fold increase in *CYP24* occurring after 1-hour incubation with 100 nmol/L $1\alpha,25(OH)_2D_3$. Expression essentially plateaued after 3 hours at 10,000- to 100,000-fold increases, compared with control, and was sustained for the duration of the analysis (16 hours). The dynamics in MDA-MB-231 cells was similar but the amplitude was considerably lower (23-fold induction after 6-hour treatment with $1\alpha,25(OH)_2D_3$ $P < 0.0001$) and thereafter reached a plateau of ~100-fold (Fig. 1A).

A similar, but not so striking, suppressed VDR responsiveness was seen with the other two gene targets, which are more directly associated with antiproliferative VDR effects (20, 34–38). *GADD45α* mRNA expression patterns in MCF-12A cells showed significant peaks at 4 hours (1.4-fold; $P < 0.05$), which was sustained up to 8 hours; after which, a subsequent 2.1-fold increase occurred at 12 hours ($P < 0.05$) and decreased thereafter. In MDA-MB-231 cells, the pattern was similar but the magnitude was suppressed at all time points, notably at the 12-hour time point (Fig. 1B). *VDUP-1* mRNA displayed a clear early peak increase after 1 hour (1.7-fold; $P < 0.05$) in MCF-12A cells but was absent in MDA-MB-231 cells, although a more modest significant peak was detected at 6 hours (Fig. 1C). In both cell lines, there were cyclical, modest, but not significant, modulation of the *VDR* at 1, 4, and 7 hours (data not shown). Together, these data suggest that both the antiproliferative and gene regulatory effects of $1\alpha,25(OH)_2D_3$ were repressed in breast cancer cell lines compared with nontumorigenic MCF-12A cells.

Expression and regulation of VDR and corepressors correlate with reduced $1\alpha,25(OH)_2D_3$ sensitivity. We hypothesized that in the cancer cell line panel, the suppressed cellular responses towards $1\alpha,25(OH)_2D_3$ (Table 1) and VDR target gene expression (Fig. 1) were determined by an altered relative ratio of the *VDR* and either one or all of the VDR interactive corepressors. We therefore compared the basal expression of *VDR*, *NCoR1*, *NCoR2/SMRT*, and *TRIP15/Alien* in malignant T47-D, ZR-75-1, MCF-7, and MDA-MB-231 to that in MCF-12A cells (Fig. 2A). T47-D cells displayed similar expression levels of *VDR* and the three corepressors compared with MCF-12A, which reflected a comparable sensitivity towards $1\alpha,25(OH)_2D_3$. In contrast, the three remaining cell lines all displayed significant reductions in *VDR*, coupled with variable changes in corepressor expression. MCF-7 and MDA-MB-231 cells had significantly elevated *NCoR1* expression (2- and 1.7-fold increase, respectively; $P < 0.05$). Interestingly, *TRIP15/Alien* was also significantly elevated in MCF-7 cells (1.8-fold; $P < 0.05$) but modestly reduced in MDA-MB-231 cells. Consequently, in the $1\alpha,25(OH)_2D_3$-resistant cancer cell lines, the ratio of *NCoR1* to *VDR* is increased compared with the normalized one in MCF-12A cells, which is arbitrarily set at 1:1. Thus, in exponentially proliferating MDA-MB-231 cells, the ratio of *NCoR1* to VDR is 14:1 (Table 2).

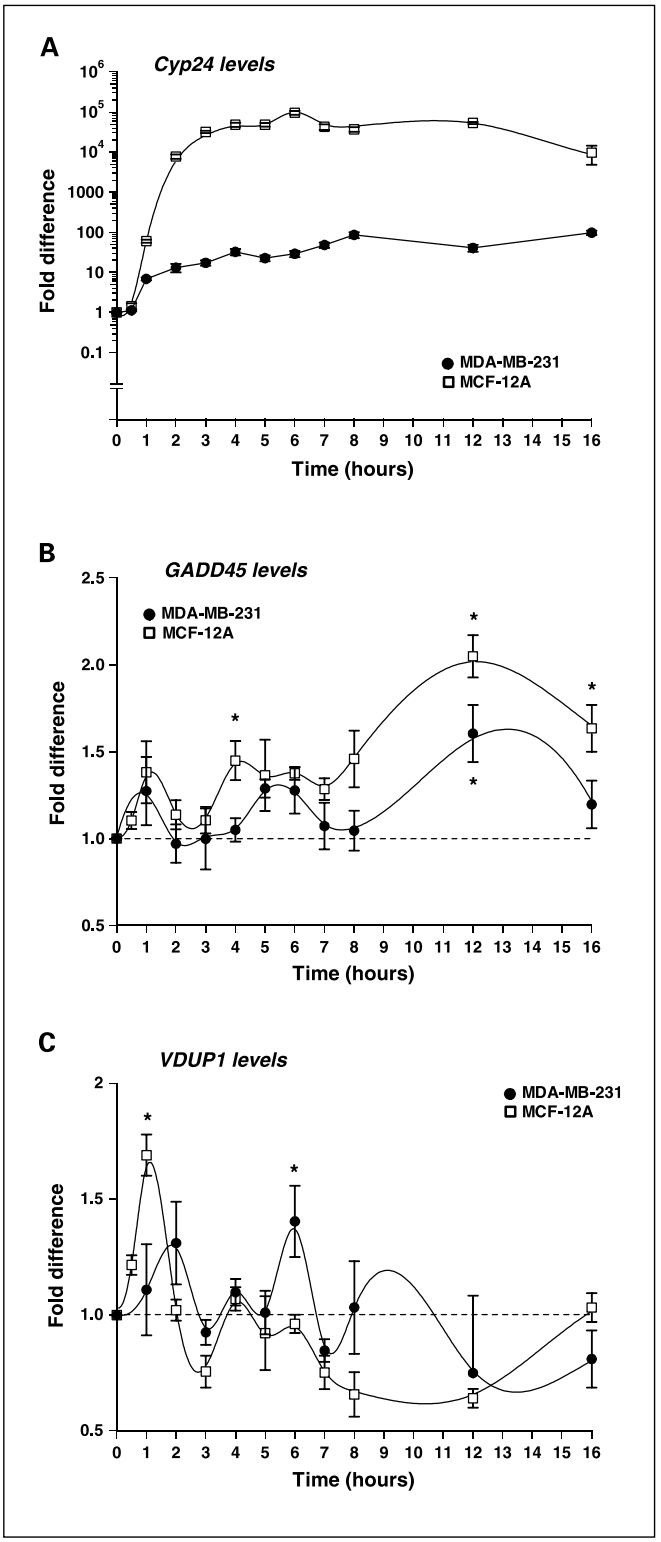

Fig. 1. Regulated levels of VDR target genes in MCF-12A and MDA-MB-231 cells treated with $1\alpha25(OH)_2D_3$. Cells ($2 \times 10^4/cm^2$) were plated into six-well plates and allowed to grow for 36 hours to ensure that cells were in mid-exponential phase. Cells were treated with $1\alpha25(OH)_2D_3$ (100 nmol/L) or left untreated (control). Total RNA was isolated after the indicated time periods, reverse transcribed, and the target genes amplified and the fold increase calculated as described in Materials and Methods. Points, mean of three separate experiments amplified in triplicate wells; bars, SE. *A, CYP24*; *B, GADD45α*. *C, VDUP-1*. *, $P < 0.05$, treatments that were significantly greater than control. All points in (*A*) were significantly different from control, and between MCF-12A and MDA-MB-231.

We sought to dissect further the dynamic expression patterns of the corepressors relative to the *VDR* and, therefore, we investigated the expression profiles in the four cancer cell lines under differing proliferation conditions. Cell cycle analyses confirmed that subconfluent cultures were associated with increased proportions of actively dividing cells as revealed by an increased percentage of cells in either S or G_2-M phase. For example, subconfluent MCF-7 cultures had 43 ± 2.3% of cells in G_1 and, on confluence, this was significantly increased to 62 ± 3.4% ($P < 0.05$). Subconfluent MDA-MB-231 cultures had 38 ± 1.7% of cells in G_1 and, on confluence, this was significantly increased to 60 ± 4.2% ($P < 0.05$). Similar patterns were seen in T47-D and ZR-75-1 (data not shown). These effects were confirmed with elevated cyclin E levels in subconfluent versus confluent cultures (Fig. 2B).

T47-D cells displayed a clear, significant reduction in the levels of *NCoR1* and *TRIP15/Alien* mRNA at confluence (0.6- and 0.5-fold reduction, respectively, relative to same cell exponential controls; $P < 0.05$; Fig. 2C). MDA-MB-231 cells, which had significantly higher basal levels of *NCoR1* compared with exponentially proliferating T47-D cells, displayed no down-regulation of *NCoR2/SMRT*, *NCoR1*, or *TRIP15/Alien* mRNA in confluent compared with subconfluent cultures. However, comparable analyses in MCF-7 cells revealed a significant reduction in *NCoR1* (0.7-fold; $P < 0.05$) on confluence (Fig. 2C). Viewed in this way, the graded ability to regulate corepressors, and in particular *NCoR1*, also correlates closely with $1\alpha,25(OH)_2D_3$ sensitivity (Table 2; Fig. 2C). Together these data support a model where *NCoR1* is up-regulated in cells and this level is sustained, irrespective of proliferation status, in the most $1\alpha,25(OH)_2D_3$ recalcitrant cells.

Corepressors are elevated in ERα-negative tumors. To investigate further the significance of deregulated corepressor expression in breast cancer, we examined 21 matched tumor and normal breast cancer samples. To allow for epithelial enrichment in the tumor samples, the relative levels of corepressors were normalized to *cytokeratin 19* mRNA, an established marker of mammary epithelial cells (39). There was considerable variation in the level of the *VDR* in both the ERα-positive (14 of 21) and ERα-negative (7 of 21) tumors with a mean fold change of 4.9 ± 2.1 and 11.8 ± 7.3, respectively, compared with the matched normal, although there was significant variation (Fig. 3A).

These data were then transformed further by normalizing the corepressor expression data to the level of *VDR* in tumor sample to reveal the ratios of corepressor to *VDR*, which are shown in Fig. 3B to D. This ratio was noticeably increased in the ERα-negative tumors whereas it was decreased in the ERα-positive tumors. Thus, the mean ratio of the *NCoR1* to *VDR* was 0.25 ± 0.1:1 in the ERα-positive tumors and 4.2 ± 1.4:1 in the ERα-negative tumors, with similar changes in the ratios of *SMRT/NCoR2* and *TRIP15/Alien* to *VDR*. Interestingly, the level of either *NCoR1* or *SMRT/NCoR2* positively correlated with the *VDR* [$R^2 = 0.45$ and 0.66; $P < 0.0006$ and $P < 4 \times 10^{-6}$, respectively], suggesting that the levels of corepressors were coregulated with the VDR.

Targeting elevated corepressor levels in $1\alpha,25(OH)_2D_3$-insensitive cancer cell lines with histone deacetylation or methylation inhibitors. The above data indicate that corepressors are elevated in breast cancer cell lines and in primary cancer tissue, notably in ERα-negative tissue. Furthermore, at least in cell lines, deregulation of *NCoR1* expression correlates with diminished responsiveness to $1\alpha,25(OH)_2D_3$. These data suggest that elevated levels of corepressors may inappropriately sustain acetylation of histone lysine residues and thereby

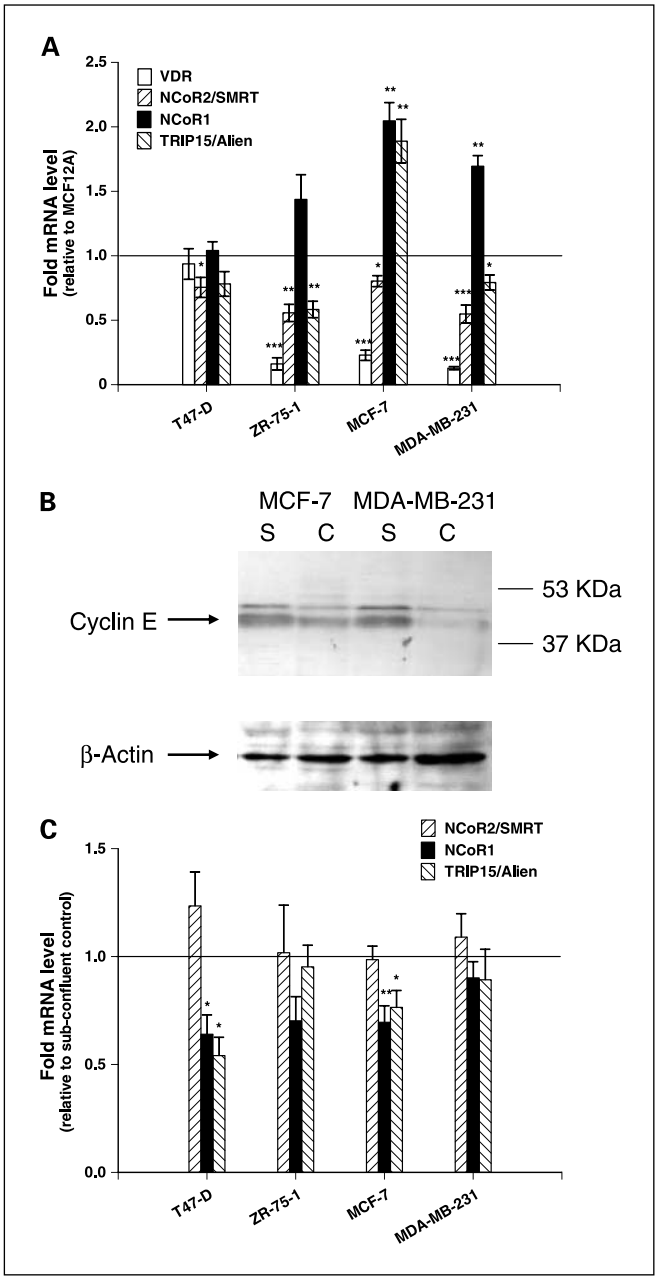

Fig. 2. Fold elevation of nuclear corepressor mRNA levels in breast cancer cell lines. *A, VDR* and corepressor mRNA levels measured by quantitative reverse transcription-PCR in T47-D, ZR-75-1, MCF-7, and MDA-MB-231 compared with MCF-12A nonmalignant breast epithelial cells. Total mRNA was isolated from triplicate cultures in mid-exponential phase, reverse transcribed, and the target genes amplified in triplicate as described in Materials and Methods. *, $P < 0.05$; **, $P < 0.01$; ***, $P < 0.001$. *B,* protein was isolated from parallel subconfluent (*S*) and confluent (*C*) MCF-7 and MDA-MB-231 cells (Materials and Methods) and resolved by SDS-PAGE and probed with antibody to cyclin E. Representative blots are shown with the position of the proteins indicated on the left. Blots were subsequently stripped and reprobed for β-actin. *C,* the fold reduction in the mRNA levels of *NCoR1, NCoR2/SMRT*, and *TRIP15/Alien* was measured in confluent cultures of T47-D, ZR-75-1, MCF-7, and MDA-MB-231, compared with subconfluent controls, by quantitative reverse transcription-PCR. Points, mean of three separate experiments amplified in triplicate wells; bars, SE.

Table 2. Combinations of vitamin D_3 compounds plus either TSA or Aza enhance antiproliferative responses in breast cancer cells

Breast epithelial cell line	Ratio of *NCoR1* to *VDR*	$1\alpha,25(OH)_2D_3$			RO-26-2198		
		TSA	5-Aza-dCyd	TSA + 5-aza-dCyd	TSA	5-Aza-dCyd	TSA + 5-aza-dCyd
MCF-12A	1:1	P: 63 ± 8 O: 56 ± 5	P: 65 ± 7 O: 38 ± 5 *P* < 0.05	P: 75 ± 6 O: 67 ± 2 *P* < 0.05	P: 48 ± 4 O: 52 ± 5	P: 52 ± 4 O: 35 ± 5 *P* < 0.05	P: 66 ± 4 O: 68 ± 5
T-47D	1.2:1	P: 37 ± 4 O: 47 ± 5	P: 28 ± 4 O: 33 ± 6	P: 43 ± 7 O: 56 ± 6	P: 45 ± 3 O: 52 ± 6	P: 47 ± 7 O: 39 ± 3	P: 55 ± 8 O: 62 ± 4
ZR-75-1	9:1	P: 18 ± 7 O: 22 ± 6	P: 12 ± 7 O: 24 ± 6	**P: 21 ± 4** **O: 35 ± 6** *P* < 0.05	**P: 16 ± 6** **O: 33 ± 4** *P* < 0.005	**P: 5 ± 1** **O: 15 ± 5** *P* < 0.01	**P: 17 ± 6** **O: 35 ± 5** *P* < 0.05
MCF-7	1 1:1	P: 29 ± 4 O: 30 ± 5	P: 28 ± 4 O: 34 ± 6	P: 43 ± 3 O: 51 ± 3	P: 25 ± 4 O: 29 ± 2	**P: 25 ± 2** **O: 42 ± 3** *P* < 0.001	**P: 40 ± 3** **O: 55 ± 2** *P* < 0.002
MDA-MB-231	14:1	P: 26 ± 2 O: 35 ± 8	P: 14 ± 2 O: 9 ± 3	P: 48 ± 3 O: 41 ± 5	**P: 41 ± 4** **O: 61 ± 2** *P* < 0.001	P: 29 ± 4 O: 36 ± 6	P: 63 ± 5 O: 55 ± 6

NOTE: $1\alpha,25(OH)_2D_3$ or RO-26-2198 (100 nmol/L) was combined with TSA (25 nmol/L for MCF-12A and 15 nmol/L for cancer cell lines) or 5-aza-dCyd (250 nmol/L). Proliferation inhibition was measured in liquid media after 96 hours, with redosing after 48 hours. The predicted (P) values represent the inhibition of vitamin D_3 compound alone added to the inhibition from TSA alone, 5-aza-dCyd alone, or TSA with 5-aza-dCyd together. The observed (O) values represent the actual inhibition of proliferation obtained. All experiments were carried out thrice independently in triplicate wells. Interactions are represented as follows: bold type, strong additive; normal type, additive; shaded box, subadditive.

reduce the ability of the VDR to initiate transcription. Histone deactylation leading to chromatin condensation has been shown to form a template for DNA methyltransferases to initiate a more stable long-term silencing of gene loci (40–42). Therefore, we reasoned that the relative $1\alpha,25(OH)_2D_3$ insensitivity associated with elevated *NCoR1* could be countered by cotreatment with minimally active ED_{25} doses of the histone deacetylation inhibitor (TSA) and the DNA methyltransferase inhibitors (5-aza-dCyd), either alone or in combination with vitamin D_3 compounds.

Furthermore, a limitation of $1\alpha,25(OH)_2D_3$ function is its rapid metabolism by the catabolic enzyme 24-hydroxylase, encoded by the VDR target gene *CYP24*, and therefore we and others have synthesized a range of vitamin D_3 analogues which are protected from 24-hydroxylase–mediated metabolism. Thus, RO-26-2198 (27, 28) was used to control for the 24-hydroxylase metabolism of ligand. Then, we undertook a comprehensive profile of combinatorial effects against MCF-12A and a panel of breast cancer cell lines using combinations of vitamin D_3 compounds [$1\alpha,25(OH)_2D_3$ or RO-26-2198 (100 nmol/L)] with TSA and 5-aza-dCyd, either alone or together.

These studies revealed that generally the strongest individual agent effects were observed in MCF-12A cells. That is, whereas MCF-12A cells were potently inhibited by each agent individually, they did not display any significant co-operativity. Indeed, with a few cotreatments (e.g., with vitamin D_3 compounds plus 5-aza-dCyd), the observed effects were actually significantly suppressed compared with the predicted effects. By contrast, there was enhancement of observed over predicted effect by cotreatment with TSA in the cancer cell line models. Importantly, the extent of the co-operative interactions correlated with the altered ratio of *NCoR1* to *VDR* and was most pronounced in the ERα-negative cell line MDA-MB-231. Thus, combinations of RO-26-2198 with TSA were additive in T47-D, whereas in ZR-75-1 and MDA-MB-231, these effects were converted to strong additive interactions (Table 2).

Changes in cell cycle distribution associated with vitamin D_3 compounds plus TSA treatments. The antiproliferative actions of vitamin D_3 in various cell models have been associated with induction of G_1 cell cycle arrest and/or induction of apoptosis (18, 43, 44), and we examined the extent to which MCF-12A cells displayed either of these responses. After 24-hour exposure to $1\alpha,25(OH)_2D_3$ (100 nmol/L), there was a significant accumulation of cells in G_1 (62 ± 4%; $P < 0.05$) compared with 43% in G_0-G_1 in matched mid-exponentially proliferating control cells and a concomitant reduction in the proportion of cells in S and G_2-M phase. In parallel, we measured changes in mitochondrial membrane integrity using JC-1 dye, which dimerizes and fluoresces red in healthy mitochondria compared with monomeric green when membrane potential is lost. This approach measures the early commitment of cells toward apoptosis and therefore was examined at 24 and 48 hours using previously optimized protocols (21). These analyses found only minor, nonsignificant changes, which suggested that the cells were not undergoing apoptosis (data not shown).

Subsequently, we measured the extent to which cotreatments of vitamin D_3 compounds plus TSA altered the cell cycle profile in MCF-12A, MCF-7, or MDA-MB-231 cells. The cotreatment with TSA in MCF-12A cells did not enhance the clear effect of $1\alpha,25(OH)_2D_3$ alone. By contrast, the cancer cell lines showed the clearest changes in cell cycle distribution with vitamin D_3 compounds and TSA cotreatment. Thus, mid-exponentially proliferating control MCF-7 cells displayed 42% (±1.1%) in G_1 and 21% (±1.2%) in G_2-M phase. A single treatment with

either $1\alpha,25(OH)_2D_3$ or RO-26-2198 had no significant effect by 24 hours whereas only the combination of RO-26-2198 plus TSA resulted in a significant reduction of cells in G_2-M phase to 16% ($\pm$0.5%; $P < 0.01$). A similar pattern was observed in MDA-MB-231 cells where the cotreatments resulted in the clearest accumulation in G_1 and loss of cells in G_2-M. Thus, mid-exponentially proliferating control cells displayed 38% ($\pm$3.0%) in G_1 and 25% ($\pm$2%) in G_2-M phase. RO-26-2198 plus TSA resulted in 44% ($\pm$2%) of cells in G_1 and 17% ($\pm$1%) in G_2-M phase ($P < 0.05$). G_1 accumulation with RO-26-2198 plus TSA was greater still after 72 hours [50% ($\pm$2.3%)] whereas the control cells displayed an accumulation of 38% ($\pm$1.5%). Together these data suggest that the cotreatment with agents facilitates co-operative changes in the distribution of the cell cycle, which, in part, contribute to the potency antiproliferative actions.

Regulation of VDR target genes in MDA-MB-231 cells cotreated with RO-26-2198 plus TSA. In line with the hypothesis of epigenetically repressed antiproliferative target genes, we investigated the effects on the regulation of the antiproliferative target genes *GADD45α*, *VDUP-1*, and the $1\alpha,25(OH)_2D_3$-regulatory *CYP24*. Time-course studies (0-16 hours) in MDA-MB-231 cells were undertaken to investigate the effects of RO-26-2198 alone and in combination with TSA. Treatments with RO-26-2198 alone revealed that patterns and fold changes of *GADD45α*, *VDUP-1*, and *CYP24* did not significantly differ between $1\alpha,25(OH)_2D_3$ and RO-26-2198 (Figs. 1 and 4).

By contrast, cotreatment with RO-26-2198 and TSA co-operatively regulated target genes. The induction of *GADD45α* in MDA-MB-231 cells by either $1\alpha,25(OH)_2D_3$ or RO-26-2198 was characterized by a broad, but suppressed, accumulation of mRNA after 12 hours, and therefore comparable to the pattern observed in MCF-12A cells (Fig. 1B). Only cotreatment with RO-26-2198 and TSA enhanced the magnitude of the 12-hour peak, resulting in a 2.4-fold increase, which was significantly greater than treatment with either RO-26-2198 or TSA alone ($P < 0.05$; Fig. 4A). Interestingly, this level was comparable to the induction in MCF-12A cells treated with $1\alpha,25(OH)_2D_3$ alone (Fig. 1B). *VDUP-1* induction also showed significant enhancement of mRNA accumulation when cotreated with RO-26-2198 plus TSA, notably at 12 hours (2.1-fold versus 1.1- and 1.6-fold for cotreatment versus TSA and RO-26-2198, respectively; $P < 0.05$; Fig. 4B).

In contrast to these effects, RO-26-2198 cotreatment with TSA had a complex range of effects on the induction of CYP24. TSA alone had little effect, but at early time points (<5 hours), it squelched RO-26-2198-mediated induction very significantly. For example, at 3 hours, the induction by RO-26-2198 alone was 14.8-fold and TSA significantly reduced this to 6.4-fold ($P < 0.0001$; Fig. 4C). At later time points, the patterns were reversed and cells cotreated with TSA plus RO-26-2198 displayed significantly enhanced CYP24 mRNA levels ($P < 0.0001$) compared with either agent alone (data not shown).

Discussion

The current study has shown that the spectrum of reduced $1\alpha,25(OH)_2D_3$-responsiveness between nonmalignant breast epithelial cells and cancer cell lines was not determined solely by a linear relationship between the levels of $1\alpha,25(OH)_2D_3$ and *VDR*. Rather, elevated levels of corepressors, such as *NCoR1*, in breast cancer cell lines and primary tumors were common and associated with insensitivity towards $1\alpha,25(OH)_2D_3$. In turn, the NCoR1 complex was targeted by cotreatments of vitamin D_3 compounds plus histone deacetylation inhibitors, which was associated with increased gene regulatory actions and antiproliferative responses.

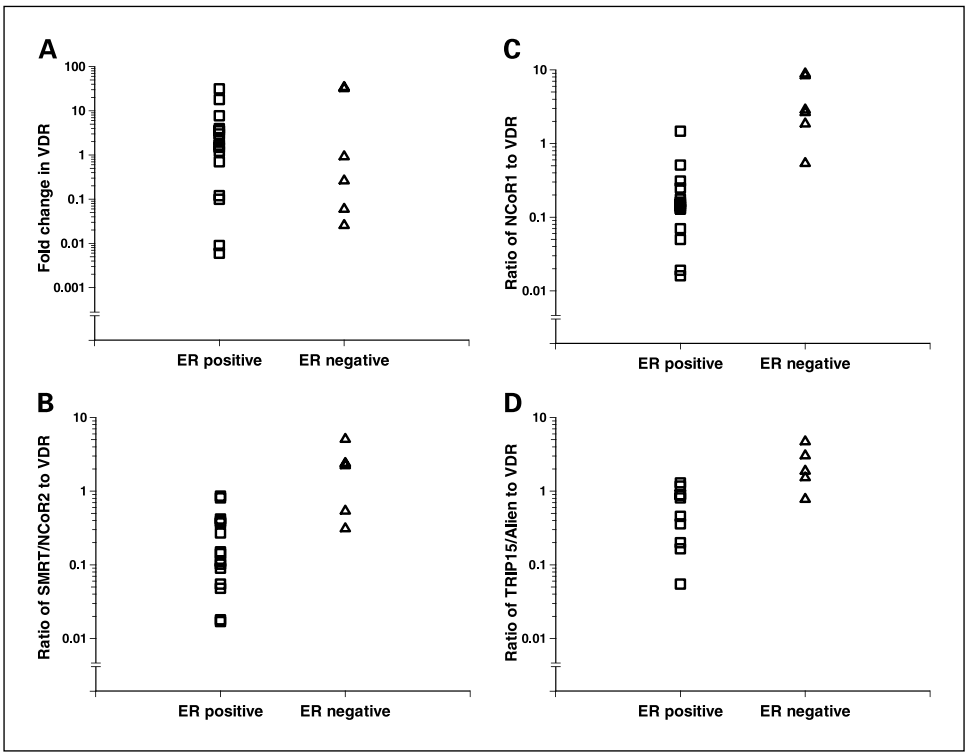

Fig. 3. Expression and altered ratio of *VDR* to corepressor mRNA levels in matched primary cultures. *A,* the relative expression of *VDR* levels in ERα-positive ($n = 14$) and ERα ($n = 7$) tumors compared with matched controls. Levels were normalized to expression of the mammary epithelial markers *cytokeratin 19*. *B* to *D,* the ratio of corepressor mRNA to *VDR*, after normalization to *cytokertain 19*, in matched tumor and normal pair as measured by quantitative reverse transcription-PCR as described in Materials and Methods.

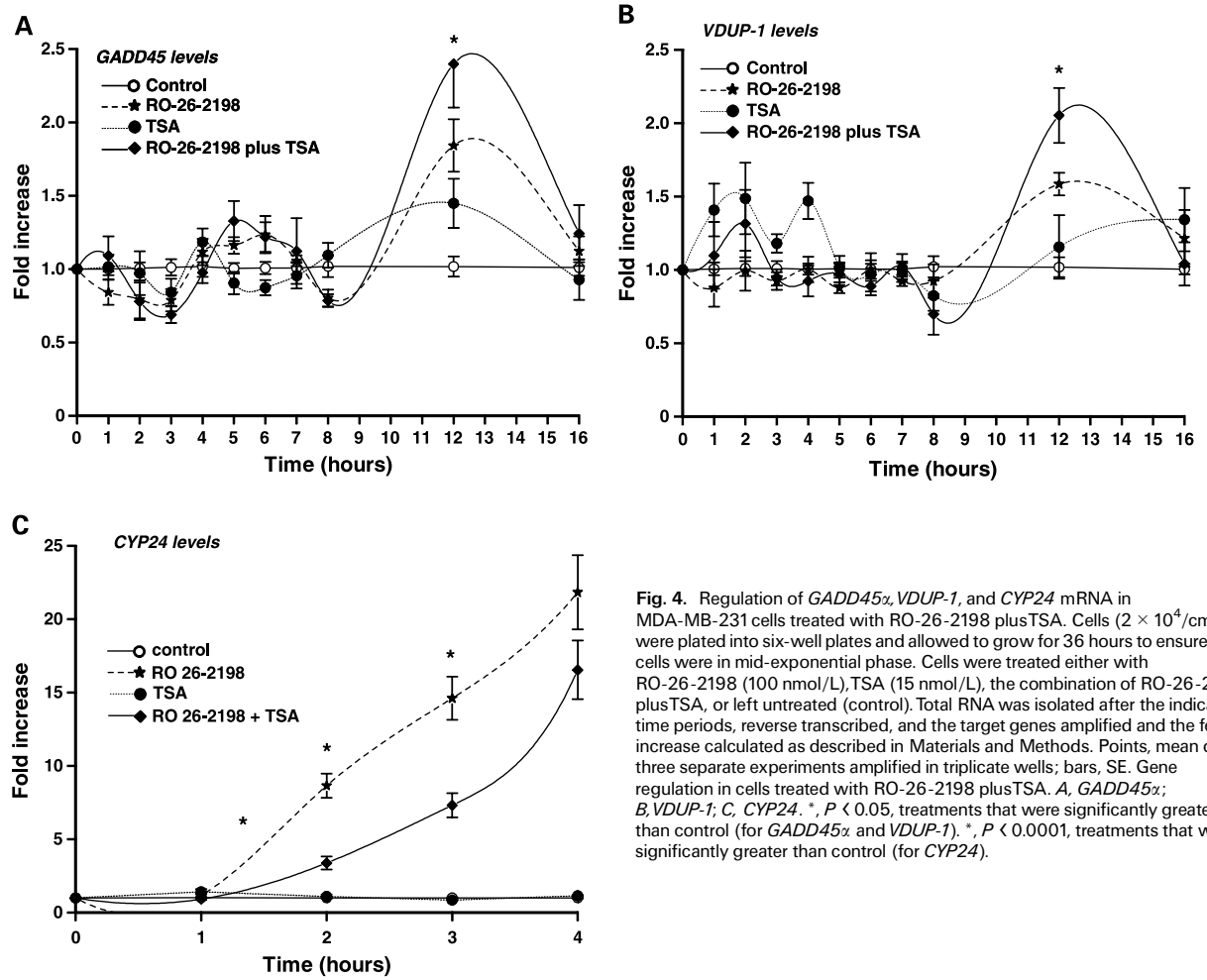

Fig. 4. Regulation of *GADD45α*, *VDUP-1*, and *CYP24* mRNA in MDA-MB-231 cells treated with RO-26-2198 plusTSA. Cells ($2 \times 10^4/cm^2$) were plated into six-well plates and allowed to grow for 36 hours to ensure that cells were in mid-exponential phase. Cells were treated either with RO-26-2198 (100 nmol/L),TSA (15 nmol/L), the combination of RO-26-2198 plusTSA, or left untreated (control). Total RNA was isolated after the indicated time periods, reverse transcribed, and the target genes amplified and the fold increase calculated as described in Materials and Methods. Points, mean of three separate experiments amplified in triplicate wells; bars, SE. Gene regulation in cells treated with RO-26-2198 plusTSA. *A, GADD45α; B, VDUP-1; C, CYP24*. *, $P < 0.05$, treatments that were significantly greater than control (for *GADD45α* and *VDUP-1*). *, $P < 0.0001$, treatments that were significantly greater than control (for *CYP24*).

VDR target gene regulation studies revealed that each gene target seemed to have a distinct profile of mRNA accumulation, which often differed between the malignant and nonmalignant background. The complex choreography of nuclear receptor-mediated transactivation has only recently emerged and involves cyclical rounds of receptor-coactivator complex assembly, recruitment of members of the large "bridging" DRIP/TRAP/ARC complex, which links the receptor complex to the cointegrators CREB-binding protein/p300, and basal transcriptional machinery (9, 10). In ligand-replete systems, these cycles can be transient (<30 minutes) and include the sequential assembly of receptor complexes followed by subsequent complex disassembly, proteosome-mediated receptor degradation, and/or recruitment of corepressors to remaining receptors to reconstitute repressive complexes (45, 46). More recently, it has emerged that different response elements respond to ligand in a relatively asynchronous manner with separate, temporal patterns of receptor associations with coactivators and corepressors (e.g., vitamin D response element on the promoter/enhancer region of the *CYP24* gene; ref. 47).

The pulsatile mRNA accumulation patterns of the target genes *VDUP-1* and *GADD45α* may reflect such spatiotemporal cycling recruitment of *apo* and *holo* receptor megacomplexes at individual vitamin D response element on the promoter/enhance of target genes. We propose that deregulated corepressor levels shift the dynamic equilibrium between *apo* and *holo* receptor conformations to histone deacetylation around the vitamin D response element and favor transcriptional repression. Thus, VDR gene targets (e.g., *CYP24*, *GADD45α*, and *VDUP-1*) are less responsive to $1\alpha,25(OH)_2D_3$ in MDA-MB-231 cells compared with MCF-12A cells. Somewhat paradoxically, the basal levels of *CYP24* and *VDUP-1* are elevated in MDA-MB-231 compared with MCF-12A cells, which suggests that the responsiveness, rather than the absolute expression levels, is targeted for disruption; certainly, there is a clear advantage to be gained in cancer cells by having elevated basal levels of *CYP24*, which is also a target for amplification in breast cancer (48).

Increased ratios of corepressor to *VDR* correlated with loss of sensitivity towards $1\alpha,25(OH)_2D_3$ and elevated proliferative status, suggesting that VDR responsiveness is repressed in post-G_1 cells. Corepressor down-regulation in G_1 may afford a "window" of sensitivity towards antimitotic hormones such as $1\alpha,25(OH)_2D_3$. Possibly reflective of their deregulated proliferative status, frequent corepressor up-regulation was found in ERα-negative primary tumors. Interestingly, in the primary

tumor material, *NCoR1* and *SMRT/NCoR2* levels were positively correlated with *VDR* levels. These data suggest that where the *VDR* is elevated, it may actually provide a benefit to the tumor. First, the increased ratio of *NCoR1* to *VDR* may drive *apo* receptor complexes to assemble on the promoter/enhancer region of target genes and, therefore, form a template for subsequent more stable epigenetic silencing of these regions. Second, it may allow cytoplasmic VDR actions to suppress apoptosis via nontranscriptional interactions (49). Elevation of *NCoR1* and *NCoR2/SMRT* found in the current study may in part explain the relative insensitivity of other breast cancer cell lines (BT-474, BT-20, HBL-100, and SK-BR-6) found by others (18, 50). Equally, we surveyed five known ERα-negative cell lines and found >2-fold increase in *NCoR1* expression levels in four (MDA-MB-175, BT-20, HBL100, and HMT3532) compared with T47-D cells (data not shown).

Metabolism of $1\alpha,25(OH)_2D_3$ limits VDR-mediated signaling. Consequently, we focused on a metabolically stable analogue of $1\alpha,25(OH)_2D_3$. However, the potency of this analogue was significantly enhanced further by the cotreatment with TSA, suggesting that ligand availability is not the sole rate-limiting factor in gene regulation. These studies revealed that increased ratio of corepressor to *VDR* predicted enhanced responsiveness to combinations of vitamin D_3 compounds plus TSA. These antiproliferative responses were associated with increased G_1 accumulation and reflected the acute antiproliferative response displayed by MCF-12A cells towards $1\alpha,25(OH)_2D_3$. These data are supported by our earlier preliminary study, which showed significant strong additive effects in clonogenic assays with MDA-MB-231 cells treated with $1\alpha,25(OH)_2D_3$ at doses as low as 1 nmol/L combined with TSA (51).

Cotreatment with vitamin D_3 compounds plus TSA may act to shift the equilibrium point between the *apo* and *holo* receptor complexes to favor a more transcriptionally permissive environment and facilitate transactivation, reflecting the greater metabolic stability of RO-26-2198; cotreatment with TSA significantly increased the levels of *GADD45α* and *VDUP-1*, notably at later time points. Parallel studies in prostate cancer also identified that *GADD45α* induction was repressed in androgen receptor–independent cancer models. Equally, the levels of *GADD45α* reexpression were comparable to those found in MDA-MB-231 cells and were shown to equate to a significant increase in protein levels (20). By contrast, induction of *CYP24* was initially suppressed by the cotreatment with vitamin D_3 compounds plus TSA. Other mechanisms are likely to play a part. For example, TSA may act to increase the expression of a negative regulator such as YY1, which has been shown to suppress transcription by the VDR on the CYP24 promoter (52). Presumably, the limited effect of this effect is related to the metabolism of TSA (53).

Collectively, our data support the hypothesis that the actions of the VDR are suppressed by an epigenetic mechanism, which attenuates the ability to regulate target genes. In support of this, we found that cancer cells with reduced antiproliferative sensitivity towards $1\alpha,25(OH)_2D_3$ also showed suppressed regulation of three VDR target genes, which in turn correlated with the ratios of corepressor to *VDR*. In addition, a similar spectrum of ratios was found in ERα-negative primary tumors. Sensitivity of breast cancer cell lines towards $1\alpha,25(OH)_2D_3$ could be enhanced by cotreating with histone deacetylation inhibitors, again most notably in the ERα-negative breast cancer models, underscoring the role of corepressors. This in turn was associated with reexpression of antiproliferative target genes, such as *GADD45α*, to a level that was comparable to that observed in nonmalignant models. *GADD45α* is an ideal candidate for a repressed VDR target gene (i.e., basal expression is comparable in all cell models) but regulation is suppressed in $1\alpha,25(OH)_2D_3$-insensitive cells.

From these data, we suggest a model whereby in ERα-positive disease, *NCoR1* and *NCoR2/SMRT* levels are reduced, reflected by the reduced ratio of expression to *VDR*, thereby enhancing estrogenic signaling. By contrast, ERα-negative tumors, which have arisen either *de novo* or as a result of tamoxifen treatment, are not reliant on estrogenic hormones, and instead elevation of *NCoR1* silences VDR and other antimitotic nuclear receptors. These findings reflect our previous studies in prostate cancer (20, 21). Equally these patterns will be compounded by the roles that these corepressors play in regulating other transcription factor actions (54–56). The current study adds to a growing body of data, which underscores the importance of the coactivator/corepressor milieu to determine nuclear receptor actions in physiology and pathophysiology (57–61).

Finally, these studies suggest that the VDR is not overtly disrupted by genetic or cytogenetic mechanisms in cancer, but rather epigenetic mechanisms selectively attenuate the transcriptional responsiveness. Such mechanisms most likely disrupt other receptors, resulting in reduced sensitivity to a wide range of dietary-derived macronutrient and micronutrient ligands. Thus, measurement of ratios of corepressor to receptors, such as *VDR* in tumor samples, may have significant prognostic and therapeutic value. The current study has highlighted the potential to establish novel chemotherapies centered around histone deacetylation inhibitors, such as TSA, or the clinically relevant suberoylanilide hydroxamic acid, in combination with potent dietary-derived nuclear receptor ligands, to deliver a more focused and sustained "anticancer" regimen for estrogen-independent disease.

References

1. Lal A, Lash AE, Altschul SF, et al. A public database for gene expression in human cancers. Cancer Res 1999;59:5403–7.
2. Hayashi SI, Eguchi H, Tanimoto K, et al. The expression and function of estrogen receptor α and β in human breast cancer and its clinical application. Endocr Relat Cancer 2003;10:193–202.
3. Qin C, Burghardt R, Smith R, Wormke M, Stewart J, Safe S. Peroxisome proliferator-activated receptor γ agonists induce proteasome-dependent degradation of cyclin D1 and estrogen receptor α in MCF-7 breast cancer cells. Cancer Res 2003;63:958–64.
4. Shao Z, Yu L, Shen Z, Fontana JA. Retinoic acid nuclear receptor α (RARα) plays a major role in retinoid-mediated inhibition of growth in human breast carcinoma cells. Chin Med Sci J 1996;11:142–6.
5. Xu XC, Sneige N, Liu X, et al. Progressive decrease in nuclear retinoic acid receptor β messenger RNA level during breast carcinogenesis. Cancer Res 1997;57:4992–6.
6. Elstner E, Muller C, Koshizuka K, et al. Ligands for peroxisome proliferator-activated receptor γ and retinoic acid receptor inhibit growth and induce apoptosis of human breast cancer cells *in vitro* and in BNX mice. Proc Natl Acad Sci U S A 1998;95:8806–11.
7. Li J, Wang J, Wang J, et al. Both corepressor proteins SMRT and N-CoR exist in large protein complexes containing HDAC3. EMBO J 2000;19:4342–50.
8. Fischle W, Dequiedt F, Hendzel MJ, et al. Enzymatic activity associated with class II HDACs is dependent

on a multiprotein complex containing HDAC3 and SMRT/N-CoR. Mol Cell 2002;9:45–57.

9. Hermanson O, Glass CK, Rosenfeld MG. Nuclear receptor coregulators: multiple modes of modification. Trends Endocrinol Metab 2002;13:55–60.

10. Nagy L, Schwabe JW. Mechanism of the nuclear receptor molecular switch. Trends Biochem Sci 2004;29:317–24.

11. Rachez C, Freedman LP. Mechanisms of gene regulation by vitamin D(3) receptor: a network of coactivator interactions. Gene 2000;246:9–21.

12. Zinser GM, Welsh J. Accelerated mammary gland development during pregnancy and delayed postlactational involution in vitamin D3 receptor null mice. Mol Endocrinol 2004.

13. Hiatt RA, Krieger N, Lobaugh B, Drezner MK, Vogelman JH, Orentreich N. Prediagnostic serum vitamin D and breast cancer. J Natl Cancer Inst 1998; 90:461–3.

14. Fogelman Y, Rakover Y, Luboshitzky R. High prevalence of vitamin D deficiency among Ethiopian women immigrants to Israel: exacerbation during pregnancy and lactation. Isr J Med Sci 1995;31:221–4.

15. Schondorf T, Eisberg C, Wassmer G, et al. Association of the vitamin D receptor genotype with bone metastases in breast cancer patients. Oncology 2003;64:154–9.

16. Guy M, Lowe LC, Bretherton-Watt D, et al. Vitamin d receptor gene polymorphisms and breast cancer risk. Clin Cancer Res 2004;10:5472–81.

17. Campbell MJ, Gombart AF, Kwok SH, Park S, Koeffler HP. The anti-proliferative effects of $1\alpha,25(OH)_2D_3$ on breast and prostate cancer cells are associated with induction of BRCA1 gene expression. Oncogene 2000;19:5091–7.

18. Elstner E, Linker-Israeli M, Said J, et al. 20-epi-vitamin D3 analogues: a novel class of potent inhibitors of proliferation and inducers of differentiation of human breast cancer cell lines. Cancer Res 1995;55: 2822–30.

19. Miller CW, Morosetti R, Campbell MJ, Mendoza S, Koeffler HP. Integrity of the 1,25-dihydroxyvitamin D3 receptor in bone, lung, and other cancers. Mol Carcinog 1997;19:254–7.

20. Khanim FL, Gommersall LM, Wood VH, et al. Altered SMRT levels disrupt vitamin D(3) receptor signalling in prostate cancer cells. Oncogene 2004;23:6712–25.

21. Rashid SF, Moore JS, Walker E, et al. Synergistic growth inhibition of prostate cancer cells by $1\alpha,25$ Dihydroxyvitamin D(3) and its 19-nor-hexafluoride analogs in combination with either sodium butyrate or trichostatin A. Oncogene 2001;20:1860–72.

22. Kurebayashi J, Otsuki T, Kunisue H, Tanaka K, Yamamoto S, Sonoo H. Expression levels of estrogen receptor-α, estrogen receptor-β, coactivators, and corepressors in breast cancer. Clin Cancer Res 2000;6:512–8.

23. Vienonen A, Miettinen S, Manninen T, Altucci L, Wilhelm E, Ylikomi T. Regulation of nuclear receptor and cofactor expression in breast cancer cell lines. Eur J Endocrinol 2003;148:469–79.

24. Zhang Z, Yamashita H, Toyama T, et al. NCOR1 mRNA is an independent prognostic factor for breast cancer. Cancer Lett 2005. Epub 2005 Jul 11.

25. Girault I, Lerebours F, Amarir S, et al. Expression analysis of estrogen receptor α coregulators in breast carcinoma: evidence that NCOR1 expression is predictive of the response to tamoxifen. Clin Cancer Res 2003;9:1259–66.

26. Getzenberg RH, Light BW, Lapco PE, et al. Vitamin D inhibition of prostate adenocarcinoma growth and metastasis in the Dunning rat prostate model system. Urology 1997;50:999–1006.

27. Uskokovic MR, Norman AW, Manchand PS, et al. Highly active analogs of $1\alpha,25$-dihydroxyvitamin D(3) that resist metabolism through C-24 oxidation and C-3 epimerization pathways. Steroids 2001;66: 463–71.

28. Campbell MJ, Elstner E, Holden S, Uskokovic M, Koeffler HP. Inhibition of proliferation of prostate cancer cells by a 19-nor-hexafluoride vitamin D3 analogue involves the induction of p21waf1, p27kip1 and E-cadherin. J Mol Endocrinol 1997;19:15–27.

29. Carlberg C. Ligand-mediated conformational changes of the VDR are required for gene transactivation. J Steroid Biochem Mol Biol 2004;89–90:227–32.

30. Ciesielski F, Rochel N, Mitschler A, Kouzmenko A, Moras D. Structural investigation of the ligand binding domain of the zebrafish VDR in complexes with $1\alpha,25(OH)_2D_3$ and Gemini: purification, crystallization and preliminary X-ray diffraction analysis. J Steroid Biochem Mol Biol 2004;89–90:55–9.

31. Weyts FA, Dhawan P, Zhang X, et al. Novel Gemini analogs of $1\alpha,25$-dihydroxyvitamin D(3) with enhanced transcriptional activity. Biochem Pharmacol 2004;67:1327–36.

32. Paine TM, Soule HD, Pauley RJ, Dawson PJ. Characterization of epithelial phenotypes in mortal and immortal human breast cells. Int J Cancer 1992;50: 463–73.

33. Campbell MJ, Park S, Uskokovic MR, Dawson MI, Koeffler HP. Expression of retinoic acid receptor-β sensitizes prostate cancer cells to growth inhibition mediated by combinations of retinoids and a 19-nor hexafluoride vitamin D3 analog. Endocrinology 1998; 139:1972–80.

34. Han SH, Jeon JH, Ju HR, et al. VDUP1 up-regulated by TGF-β1 and 1,25-dihydorxyvitamin D3 inhibits tumor cell growth by blocking cell-cycle progression. Oncogene 2003;22:4035–46.

35. Jeon JH, Lee KN, Hwang CY, Kwon KS, You KH, Choi I. Tumor suppressor VDUP1 increases p27kip1 stability by inhibiting JAB1. Cancer Res 2005;65: 4485–9.

36. Yang X, Young LH, Voigt JM. Expression of a vitamin D-regulated gene (VDUP-1) in untreated- and MNU-treated rat mammary tissue. Breast Cancer Res Treat 1998;48:33–44.

37. Akutsu N, Lin R, Bastien Y, et al. Regulation of gene Expression by $1\alpha,25$-dihydroxyvitamin D3 and its analog EB1089 under growth-inhibitory conditions in squamous carcinoma Cells. Mol Endocrinol 2001;15: 1127–39.

38. Jiang F, Li P, Fornace AJ, Jr., Nicosia SV, Bai W. G_2-M arrest by 1,25-dihydroxyvitamin D3 in ovarian cancer cells mediated through the induction of GADD45 via an exonic enhancer. J Biol Chem 2003; 278:48030–40.

39. Stathopoulos EN, Sanidas E, Kafousi M, et al. Detection of CK-19 mRNA-positive cells in the peripheral blood of breast cancer patients with histologically and immunohistochemically negative axillary lymph nodes. Ann Oncol 2005;16:240–6.

40. Marks P, Rifkind RA, Richon VM, Breslow R, Miller T, Kelly WK. Histone deacetylases and cancer: causes and therapies. Nat Rev Cancer 2001;1:194–202.

41. Cameron EE, Bachman KE, Myohanen S, Herman JG, Baylin SB. Synergy of demethylation and histone deacetylase inhibition in the re-expression of genes silenced in cancer. Nat Genet 1999;21:103–7.

42. Zhu WG, Lakshmanan RR, Beal MD, Otterson GA. DNA methyltransferase inhibition enhances apoptosis induced by histone deacetylase inhibitors. Cancer Res 2001;61:1327–33.

43. Campbell MJ, Reddy GS, Koeffler HP. Vitamin D3 analogs and their 24-oxo metabolites equally inhibit clonal proliferation of a variety of cancer cells but have differing molecular effects. J Cell Biochem 1997;66: 413–25.

44. Welsh J, Wietzke JA, Zinser GM, Byrne B, Smith K, Narvaez CJ. Vitamin D-3 receptor as a target for breast cancer prevention. J Nutr 2003;133:2425–33S.

45. Metivier R, Penot G, Hubner MR, et al. Estrogen receptor-α directs ordered, cyclical, and combinatorial recruitment of cofactors on a natural target promoter. Cell 2003;115:751–63.

46. Reid G, Hubner MR, Metivier R, et al. Cyclic, proteasome-mediated turnover of unliganded and liganded ERα on responsive promoters is an integral feature of estrogen signaling. Mol Cell 2003;11: 695–707.

47. Vaisanen S, Dunlop TW, Sinkkonen L, Frank C, Carlberg C. Spatio-temporal activation of chromatin on the human CYP24 gene promoter in the presence of $1\alpha,25$-dihydroxyvitamin D(3). J Mol Biol 2005; 350:65–77.

48. Albertson DG, Ylstra B, Segraves R, et al. Quantitative mapping of amplicon structure by array CGH identifies CYP24 as a candidate oncogene. Nat Genet 2000;25:144–6.

49. Vertino AM, Bula CM, Chen JR, et al. Nongenotropic, anti-apoptotic signaling of $1\alpha,25(OH)2$-vitamin D3 and analogs through the ligand binding domain (LBD) of the vitamin D receptor (VDR) in osteoblasts and osteocytes: mediation by Src, PI3, and JNK kinases. J Biol Chem 2005;280:14130–7.

50. Agadir A, Lazzaro G, Zheng Y, Zhang XK, Mehta R. Resistance of HBL100 human breast epithelial cells to vitamin D action. Carcinogenesis 1999;20: 577–82.

51. Banwell CM, O'Neill LP, Uskokovic MR, Campbell MJ. Targeting $1\alpha,25$-dihydroxyvitamin D3 antiproliferative insensitivity in breast cancer cells by co-treatment with histone deacetylation inhibitors. J Steroid Biochem Mol Biol 2004;89–90:245–9.

52. Raval-Pandya M, Dhawan P, Barletta F, Christakos S. YY1 represses vitamin D receptor-mediated 25-hydroxyvitamin D(3)24-hydroxylase transcription: relief of repression by CREB-binding protein. Mol Endocrinol 2001;15:1035–46.

53. Yoshida M, Horinouchi S, Beppu T. Trichostatin A and trapoxin: novel chemical probes for the role of histone acetylation in chromatin structure and function. Bioessays 1995;17:423–30.

54. Ahmad KF, Melnick A, Lax S, et al. Mechanism of SMRT corepressor recruitment by the BCL6 BTB domain. Mol Cell 2003;12:1551–64.

55. Jepsen K, Rosenfeld MG. Biological roles and mechanistic actions of co-repressor complexes. J Cell Sci 2002;115:689–98.

56. Jepsen K, Hermanson O, Onami TM, et al. Combinatorial roles of the nuclear receptor corepressor in transcription and development. Cell 2000;102: 753–63.

57. Hermanson O, Jepsen K, Rosenfeld MG. N-CoR controls differentiation of neural stem cells into astrocytes. Nature 2002;419:934–9.

58. Planas-Silva MD, Shang Y, Donaher JL, Brown M, Weinberg RA. AIB1 enhances estrogen-dependent induction of cyclin D1 expression. Cancer Res 2001;61: 3858–62.

59. Jiang WG, Douglas-Jones A, Mansel RE. Expression of peroxisome-proliferator activated receptor-γ (PPARγ) and the PPARγ co-activator, PGC-1, in human breast cancer correlates with clinical outcomes. Int J Cancer 2003;106:752–7.

60. Kollara A, Kahn HJ, Marks A, Brown TJ. Loss of androgen receptor associated protein 70 (ARA70) expression in a subset of HER2-positive breast cancers. Breast Cancer Res Treat 2001;67:245–53.

61. Grignani F, De Matteis S, Nervi C, et al. Fusion proteins of the retinoic acid receptor-α recruit histone deacetylase in promyelocytic leukaemia. Nature 1998; 391:815–8.

Clinical Cancer Research

Altered Nuclear Receptor Corepressor Expression Attenuates Vitamin D Receptor Signaling in Breast Cancer Cells

Claire M. Banwell, Donia P. MacCartney, Michelle Guy, et al.

Clin Cancer Res 2006;12:2004-2013.